A Multilevel Inverter Topology for Inductively-Coupled Power Transfer

John I. Rodriguez Steven B. Leeb
Laboratory for Electromagnetic and Electronic Systems
Massachusetts Institute of Technology
Cambridge, MA 02139, USA

***Abstract*— This paper describes a multilevel inverter for delivering power to a set of frequency selectable induction heating targets for stimulating temperature sensitive polymer actuators. The proposed inverter topology overcomes the capacitor voltage balancing issue common to traditional multilevel inverters. This inverter is suitable for sustained real power transfer.**

I. Background

We are developing an adaptive vibration damper capable of adjusting its natural frequency to improve damping over a range of vibration frequencies. This damper is an auxiliary spring-mass system and is sometimes called a dynamic vibration absorber (DVA) [1]. When a DVA is mechanically coupled to a vibrating mechanical structure such as an automobile engine, or a building, it creates a higher order mechanical system with at least one resonance and one anti-resonance. At the DVA's natural frequency, the total system experiences an anti-resonance where the mass of the DVA and the mass of the vibrating structure move in counterpoise. The mass of the primary mechanical structure remains relatively stationary while the DVA oscillates as a result of "absorbing" the disturbing vibration.

Typically, a DVA is designed to provide maximum damping at its fixed natural frequency. A more sophisticated DVA can adjust its natural frequency by varying its spring constant with a magnetic actuator, a material, or some other mechanical scheme [2]. Because the DVA concept applies equally well to both linear and rotational systems, we are exploring an additional approach: a DVA which can adjust its natural frequency by controlling its moment of inertia. Figure 1(a) shows a simplified model of a rotational DVA with an adjustable moment of inertia. A variable inertia, J_2, can be created using a cylindrical container filled with a gel fluid. This fluid can be created from a solution of temperature sensitive polymer gel beads suspended in a solvent. Below a certain temperature the gel beads swell, absorbing the surrounding solvent into the polymer matrix (like a sponge). When this happens the gel beads pack tightly in the container, adding significantly to the container's moment of inertia. At higher temperatures the polymer network shrinks, allowing the solvent to flow freely. This effectively decouples the gel-solvent mass and lowers the apparent rotational inertia J_2. By subdividing

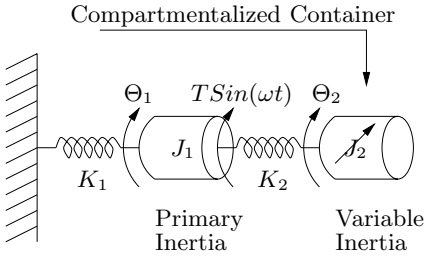

(a) DVA with variable inertia.

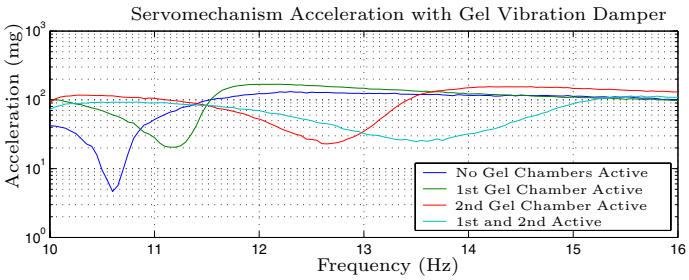

(b) Primary inertia J_1 acceleration.

Fig. 1. Simplified model of gel damper and acceleration response of primary inertia J_1.

the container into n multiple compartments of varying gel mass, 2^n anti-resonant states are made possible depending on which compartments are heated. Figure 1(b) shows peak damping at four different vibration frequencies created by a 2-compartment gel DVA prototype.

II. Frequency Selectable Induction Heating Targets

Each gel compartment must be hermetically sealed to prevent the escape of solvent. Friction must be minimized in the DVA spring-mass system to maximize the depth of the anti-resonance. It is economically and mechanically advantageous to keep the packaging of each compartment simple. Heating schemes that require contact with a gel compartment are therefore undesirable. Induction heating of the gel compartments can deliver heat without physical contact, a distinct advantage in this and other (including

0-7803-7768-0/03/$17.00 (C) 2003 IEEE

medical) applications. In the multi-compartment DVA, the induction heating system must be capable of selectively heating any combination of gel compartments.

In our prototype, each gel compartment contains an induction target that heats preferentially at one frequency with respect to the other targets. A single converter capable of driving a sum-of-sinewaves across a single "primary-side" induction coil heats the desired combination of induction targets. The frequency selective targets used in our DVA do not require a separate induction coil for each target, unlike other multi-load/single converter induction heating systems [3].

The term "induction heating" usually refers to situations where ohmic dissipation results primarily from current crowding near the conductor's surface as the result of induced eddy currents. Increasing the conductor's thickness increases the effect of magnetic shielding in the interior of the conductor. Perhaps counter-intuitively, a thin-walled conductor whose thickness is small compared to its skin depth δ can also act as a good shield. This phenomenon is explained in [4] and summarized by Fig. 2 below. Here a perfectly conducting $\supset$ - shaped conductor is driven by a sheet current $K_s = K_o sin(\omega t)$, where it is assumed that the conductor extends a very long height h in the direction perpendicular to the page. When the conductor thickness $\Delta << \delta$, the conductor can be thought of as forming a current divider with the $\supset$ - shaped perfect conductor. If conductivity-per-unit-width is defined as $G = \sigma\Delta/h$ and the inductance-per-unit-width as $L = \mu bh$ for this structure, the current through the thin wall is

$$K_{thin-wall} = \frac{j\omega LG}{1 + j\omega LG} K_o. \tag{1}$$

That is, the magnetic energy stored in the region to the right of the thin wall in Fig. 2 can be modeled as energy stored in a lumped inductor. As drive frequency increases, the effective impedance of this inductance increases, forcing a greater fraction of the drive current into the resistive sheet. This transfer function is identical in form to the output current flowing through the resistive leg of a parallel L-R circuit that is driven by a current source input. Consequently, the thin-walled conductor can be modeled as a parallel L-R circuit providing that $\Delta << \delta$.

If each target is designed to have a similar self-inductance but a different resistance, a preferential heating scheme can be devised. Consider, for example, three shorted, single-turn inductors each with a different resistance, all of which are coupled to a single "primary" induction coil driven by a sinusoidally varying current as illustrated in Fig. 3.

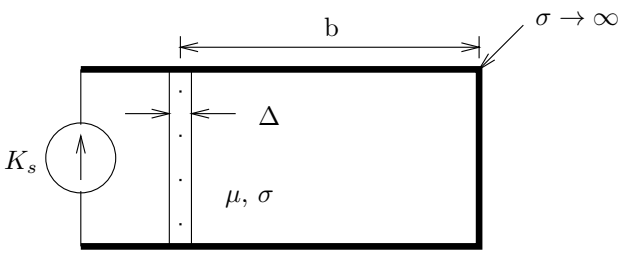

Fig. 2. Shielding in thin-walled conductors

Assuming that the cross-coupling between targets is negligible, it can be shown that the time-averaged power dissipated in target n (1,2, or 3) at its -3dB breakpoint (in Hertz)

$$f_n = \frac{R_n}{2\pi L_s} \tag{2}$$

is given by

$$< P_n >= \frac{1}{2} L_p (K_n \cdot I_p)^2 f_n, \tag{3}$$

where K_n is the coupling coefficient between the primary coil and target n. Additionally, if the resistance between two targets differs by a factor of α, i.e. $R_{n+1} = \alpha R_n$, it can be shown that the time-averaged power dissipated in R_n when driven at its breakpoint frequency is:

$$< P_n >= \frac{1 + \alpha^2}{2\alpha} \left(\frac{K_n}{K_{n+1}} \right)^2 < P_{n+1} > . \tag{4}$$

We will consider a three target system with a separation factor α=5. If a coupling coefficient, $K = 0.3$, between each target and primary coil is assumed, power delivered as a function of frequency is given by the curves in Fig. 3(b). Here the $R/(2\pi L)$ breakpoint frequencies have been chosen at 4kHz, 20kHz, and 100kHz. This plot shows that, at these particular breakpoint frequencies, the target associated with that frequency receives an amount of power that is 2.6 times greater than its neighbors.

Because of the voltage drive, absolute power decreases with frequency due to the primary coil's increasing impedance with frequency. Consequently, a greater drive voltage is needed at higher frequencies to generate a constant amplitude H-field within the induction coil. The primary-side power supply must be able to create an arbitrary sum of sinewaves chosen from combinations of the three breakpoint frequencies. Any combination of these three frequencies (plus the possibility of no drive at all) could be selected to trigger an arbitrary arrangement of compartments. A power supply that can deliver power concurrently at the required frequencies is the subject of the next section.

III. "Marx" Multilevel Inverter

A. Introduction

Multilevel converters have drawn attention for approximating sinewaves. A multilevel inverter is capable of generating more than two levels, often deriving these levels from a capacitor ladder that divides a voltage source. The three most common multilevel converter topologies include the diode-clamped, capacitor-clamped and cascade-inverters with separate DC sources [5]. Unfortunately, to

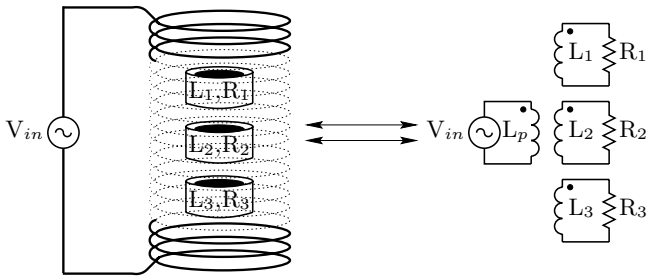

(a) Induction heating circuit.

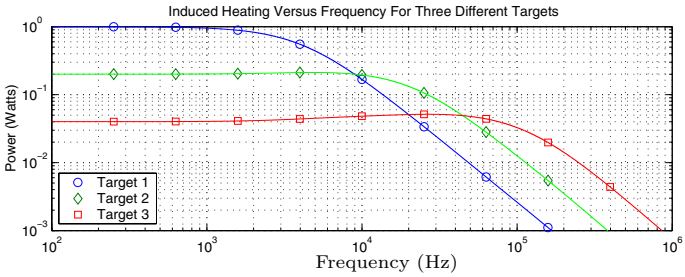

(b) Induced heating versus frequency.

Fig. 3. Induction heating circuit and power curves versus frequency for 3 different targets.

create three or more levels the first two topologies suffer from a significant capacitor voltage unbalancing problem when delivering real power [5]. In the case of a three-level converter it is possible to maintain the DC-link potential with proper control. Beyond three levels, all of these multilevel converters require separate, isolated DC sources or a complicated voltage balancing circuit for active power transfer. As a result, multilevel converters have found limited application, notably as reactive power compensators. Recently, a generalized multilevel inverter topology with self-voltage balancing was proposed [6] that overcomes the limitations of the three major topologies for levels (M) greater than 3. A drawback of this topology is that the number of active switching devices grows quadratically with the number of levels. The generalized topology is useful for inferring other possible multilevel inverters that are less part intensive – one such topology is presented here.

B. Principle of Operation

The proposed multilevel topology is based on a high voltage pulse circuit, known as a Marx Generator (Erwin Marx, 1924). The basic idea behind the Marx Generator is that it can produce a high voltage pulse by *charging a bank of capacitors in parallel and discharging them in series.* Connecting the capacitors in series is accomplished by a switching network originally comprised of spark gaps or avalanche type devices. When the first gap is triggered

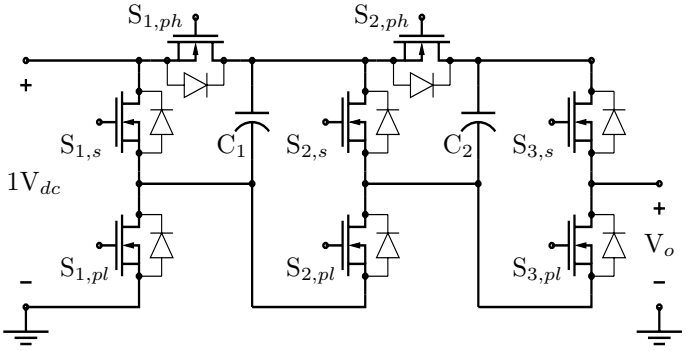

Fig. 4. A four-level Marx inverter.

it sets into motion a cascade effect whereby each successive gap fires and all the capacitors are serially discharged. If these spark gaps are replaced by controllable switching devices it becomes possible to control the number of capacitors that are serially connected to the load. The result is a multilevel topology that generates required voltage levels by multiplying the DC bus voltage as opposed to dividing it down. Because the underlying principle behind this inverter is similar to the Marx Generator, we will refer to this topology as the "Marx" multilevel inverter. Figure 4 shows an example of a single phase, M=4, Marx multilevel inverter.

An M level Marx inverter can be decomposed into a cascade of M-2 Marx cells and one half-bridge inverter. Operation of this inverter can be understood by examining the basic Marx cell shown in Fig. 5(a). Each cell is composed of a capacitor and three switches which serve to either parallel (via $S_{m,pl}$,$S_{m,ph}$) the capacitor with the cell preceding it or to connect it in series (via $S_{m,s}$) with it. When paralleled the output voltage of the m^{th} cell is

$$V_{m+1} = V_m, \tag{5}$$

or when in series given by

$$V_{m+1} = V_m + 1V_{dc}. \tag{6}$$

By definition $V_1 = 1V_{dc}$. The cascade of Marx cells can be used to generate M-1 levels above ground while the final stage shown in Fig. 5(b) is used to select one of these levels to produce

$$V_a = V_{M-1}, \tag{7}$$

or alternatively to select ground when all of the capacitors are in parallel,

$$V_a = V_{M-1} - 1V_{dc} = 0. \tag{8}$$

In general an M-level Marx inverter has 2^{M-1} possible switching states. Therefore, there are redundant states for some of the intermediate voltage levels. In the case of certain multilevel inverters, such as the capacitor-clamped topology, redundant switching states maybe useful for capacitor voltage balancing. Because the capacitor voltages

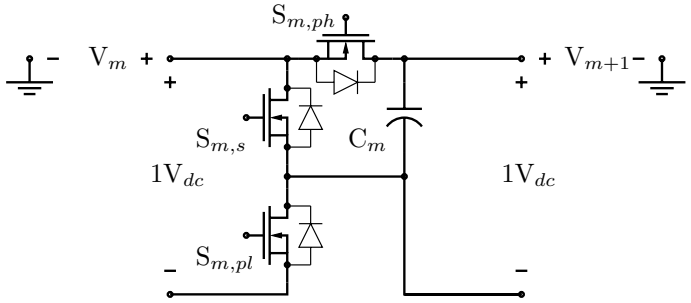

(a) Marx cell.

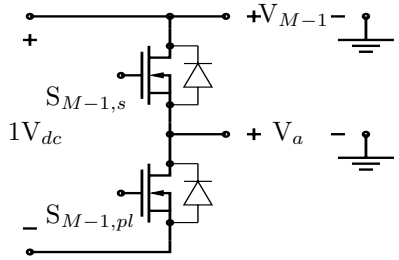

(b) Half-Bridge (M^{th} stage).

Fig. 5. The basic Marx cell and last stage half-bridge inverter.

of a Marx inverter are equalized to the bus voltage whenever all the capacitors are paralleled, redundant states need not be used. Instead, it is easier to use a set of states that simplifies the overall control. One scheme to do this is to stack the capacitors sequentially by starting from the source side. The switching states for this approach are shown in Table I. Alternatively, Fig. 6 illustrates each of these four switching patterns by depicting each on-switch in black, and each off-switch in gray.

TABLE I
A four-level Marx inverter switching states.

$\mathbf{V_a}$	$\mathbf{S_{1,p}}$	$\mathbf{S_{2,p}}$	$\mathbf{S_{3,p}}$	$\mathbf{S_{1,s}}$	$\mathbf{S_{2,s}}$	$\mathbf{S_{3,s}}$
$0V_{dc}$	1	1	1	0	0	0
$1V_{dc}$	0	0	1	1	1	0
$2V_{dc}$	0	1	1	1	0	0
$3V_{dc}$	1	1	1	0	0	0

C. Control and Modulation Strategy

Most control and modulation strategies for multilevel inverters are meant for synthesizing sinewaves at low frequencies for utility or industrial applications. In general these approaches fall into two categories [10]:

- High switching frequency PWM techniques.
- Fundamental switching frequency techniques

Two high frequency PWM methods, the classic sinusoidal PWM method and the Space Vector PWM approach,

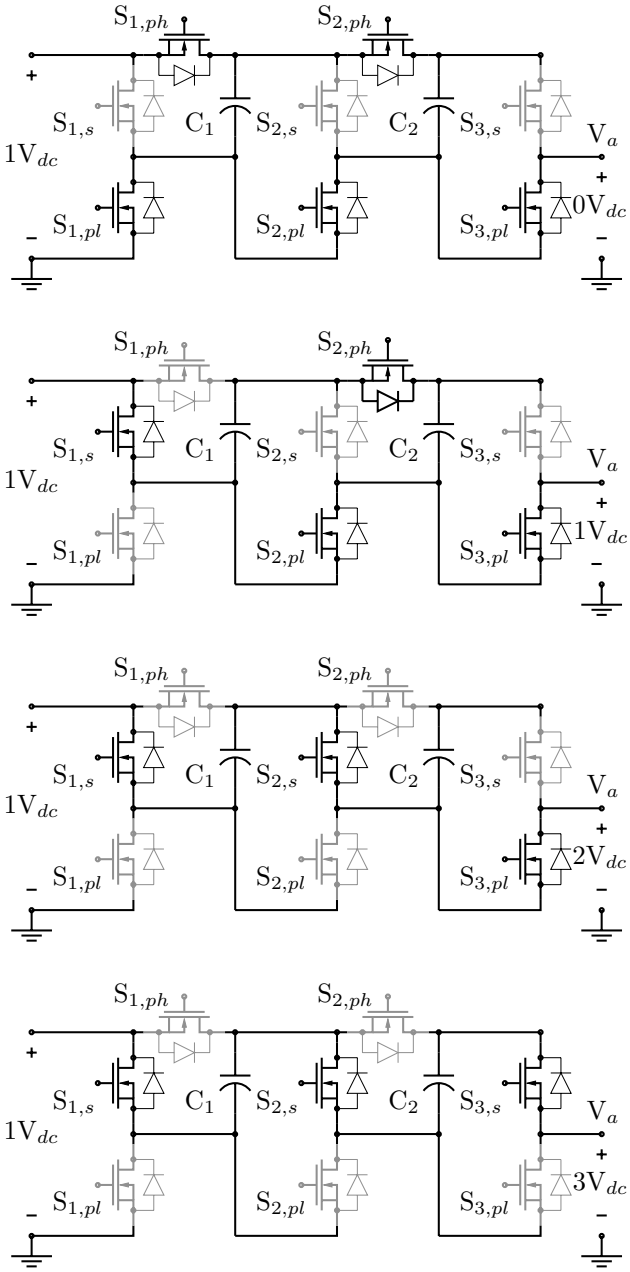

Fig. 6. A four-level Marx inverter switching states.

are well-suited to low frequency sine generation. These schemes suffer from significant switching losses as well as switching speed limitations when trying to synthesize sinewaves in the 100-300 kHz range or higher. For high frequencies, fundamental switching frequency strategies can be advantageous, generally requiring fewer switching transitions to produce a sinusoidal approximation. A conventional 6-pulse sinewave drive is a familiar example of a fundamental switching frequency technique. Recent fundamental switch frequency strategies include the selective harmonic elimination approach[14] and the Space Vector Control technique [11].

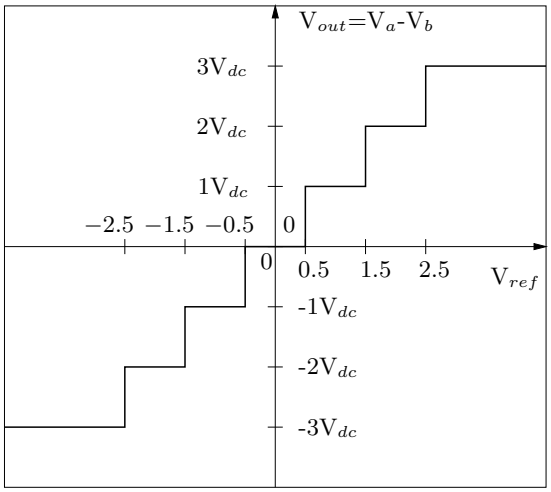

Fig. 7. A 7-level symmetric uniform mid-tread quantizer.

We are examining a different fundamental switching frequency strategy – using the Marx inverter as a symmetric uniform quantizer. This approach can be implemented with a minimal amount of analog hardware, is simple to understand, and can be used to approximate more complicated AC waveforms (such as a sum of three sinewaves). This makes the Marx inverter suitable for driving multiple targets in our induction heating example. Hardware implementation consists of a bank of comparators that converts the reference waveform into a simple thermometer code, not unlike those used in flash analog-to-digital converters. The output is then decoded (with an appropriate amount of inserted dead-time) to provide the correct gate drive logic for two M=4, single-phase Marx inverters operated differentially. This creates a 7-level, symmetric uniform mid-tread quantizer whose transfer characteristic is shown in Fig. 7.

Figure 8 is a collection of sample waveforms generated by a 1KW prototype Marx inverter functioning as a 7-level quantizer. Two M=4 phase legs are used to drive either a 200μH air coil inductor Fig. 8(a-c) or a 100Ω resistor Fig. 8(d) differentially. Each snapshot shows three waveforms which correspond (from top to bottom) to the input reference waveform, a multilevel approximation and the current drawn from the converter. As seen in these various scope plots, the Marx inverter can drive a variety of AC waveforms into an inductive load, and/or deliver real power while still maintaining appropriate voltage levels.

IV. Performance Comparison: PWM Full-Bridge VSI vs. Quantized Marx VSI

The Marx inverter is a component-intensive solution in comparison to a simple full-bridge inverter. The decision to choose this converter as a viable solution must be justified on the basis of performance versus economic trade-off. We will consider two benchmarks for circuits designed to synthesize power-level sinewaves:

1) The quality of the generated sinewave at the output.
2) The converter's internal loss mechanisms.

The first benchmark is measured by examining the total harmonic distortion (THD) present in the load current. In this case the distortion in the current is determined by

$$THD = \sqrt{\frac{I_{rms}^2 - I_{rms,1}^2}{I_{rms,1}^2}}, \tag{9}$$

where I_{rms} is the rms value of the load current and $I_{rms,1}$ is the rms value of the load current's fundamental component. The PWM Full-Bridge VSI, shown in Fig. 9, is a prime candidate for comparison against the quantized Marx inverter because of its popularity and simplicity. There are also a number of PWM strategies that could be used for comparison and include, but are not necessarily limited to, the naturally sampled, symmetric and asymmetric regular sampled schemes [15]. The naturally sampled strategy is the traditional analog scheme that determines the switching instances by comparing a sine reference against a high frequency triangle waveform. The other two schemes are digital approaches. Our comparison will be confined to the naturally sampled case since the proposed control for the Marx inverter is also analog.

There are number of digital implementations that would allow for selective harmonic cancellation and hence improved performance in either type of converter. The analysis in this paper is a fair starting point for comparison. Depending on the implementation, a full-bridge can be made to produce either a bipolar or unipolar naturally sampled PWM waveform [9]. The unipolar pattern differs from the bipolar because it uses a 180^o phase-shifted version of the reference sine for determining the switching instants of the second phase leg. For clarity, Fig. 10 shows an example of a naturally sampled unipolar PWM scheme were the modulation frequency has been arbitrarily chosen to be seven times faster than the carrier frequency. The unipolar pattern minimizes low frequency harmonic content for the full-bridge PWM inverter, and will be used here as a standard for comparison.

A. Total Harmonic Distortion Comparison

Ultimately, the goal is to drive a collection of induction targets, each at it's own respective $R/(2\pi L)$ breakpoint. Before examining the multi-target case in its entirety, consider a simpler load: a resistive load, R, with a series inductor, L, for filtering. Such a circuit could be used to model a single induction target. The load current's THD over a normalized fundamental output voltage range was computed using MATLAB for both converters, with results shown in Fig. 11. In this plot, the PWM frequency modulation ratio is M_f=10 (i.e., the PWM switch frequency is 10 times the frequency of the synthesized sinewave) and a 2-phase Marx inverter is used to form a 7-level symmetric uniform quantizer. Both the quantized Marx and PWM waveforms have fundamental frequencies at the $R/(2\pi L)$ frequency of the load. As can be seen in Fig. 11, the

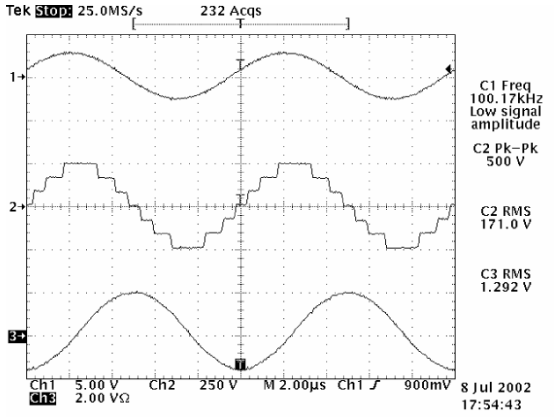

(a) 100kHz Sinewave, inductive load.

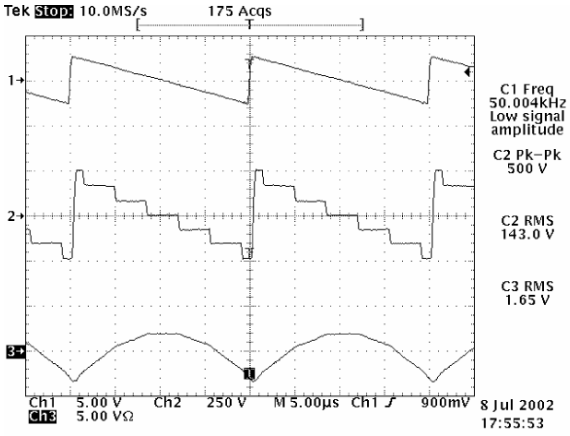

(b) 50khz Sawtooth, inductive load.

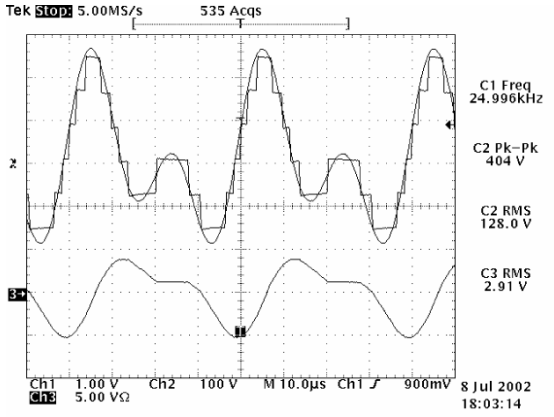

(c) Sum of sinewaves (25khz, 50khz), inductive load.

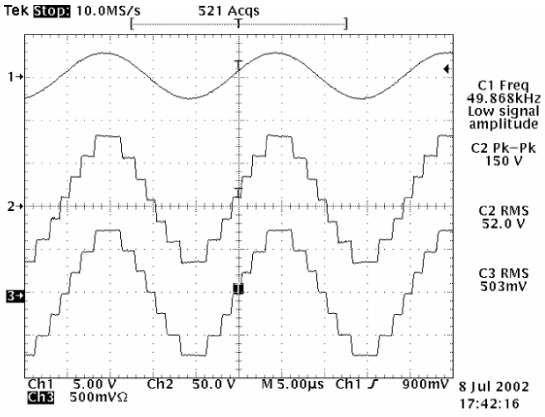

(d) 50khz Sinewave, resistive load.

Fig. 8. Marx inverter waveforms.

quantized waveform generally gives lower THD over the upper two-thirds of the achievable amplitude range. In fact over most of this range the percent THD is under 10%. Because the total delivered power can be expressed as

$$P = (1 + THD^2) I_{rms,1}^2 R, \tag{10}$$

the THD is also useful for determining how much of the total power is the result of additional harmonics. For a percent THD of less than 10%, less than 1% of the delivered power is carried by the higher current harmonics. Note that below this amplitude range, only one level of the Marx converter is being exercised and therefore the amount of harmonic distortion grows rapidly.

In the previous, single target case it was easy to see that for $M_f = 10$, the Marx output still gave better THD, at least over a useful range of output voltages. Such conclusions are not as easy to draw in the case of multiple targets, where the THD in all loads must be considered

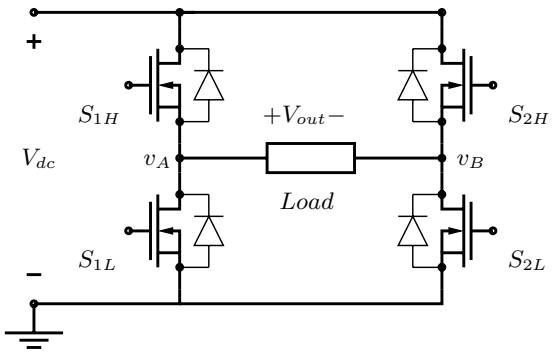

Fig. 9. Full-Bridge inverter.

simultaneously. Consider once more the multiple target system shown in Fig. 3. Recall that the separation between breakpoint frequencies is designed to be a fixed number and that the greater the separation factor α, the greater

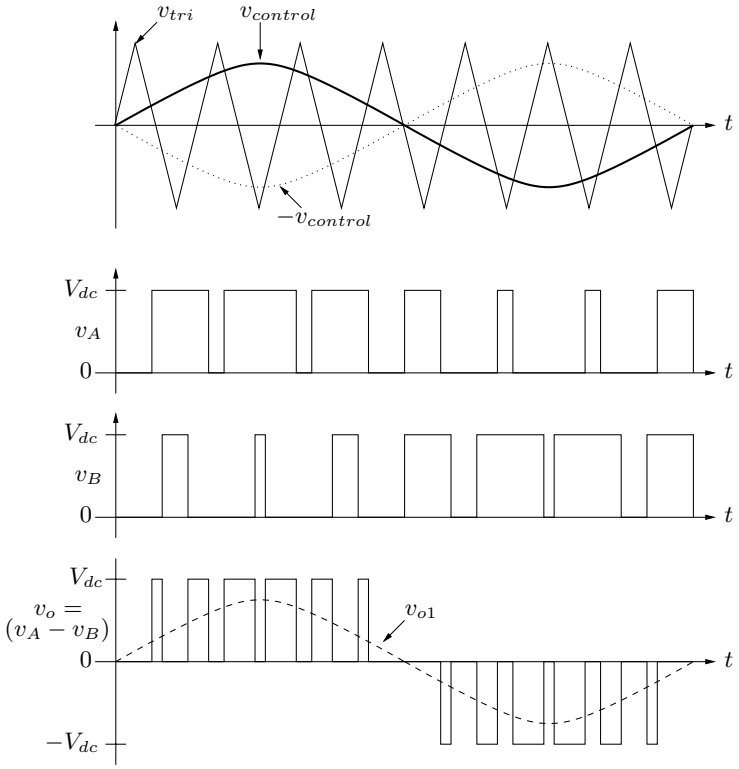

Fig. 10. Unipolar switching scheme.

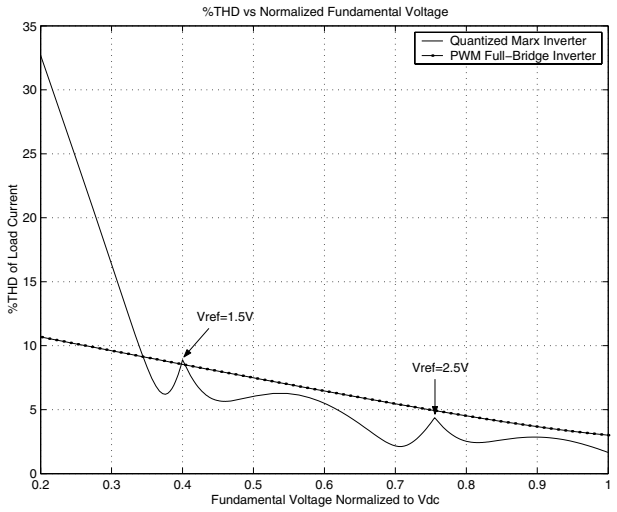

Fig. 11. Total Harmonic Distortion for a single L-R load.

the relative heating in a target. In order for this scheme to be successful, the amount of excess power delivered as a result of harmonics *to loads not intentionally driven* must be minimized.

Therefore, in the case of the multi-target load, a useful measure of converter performance is how much the additional harmonics impact the relative heating factor of a target. The theoretical relative heating factor for the sample case illustrated in Fig. 3 was calculated using MATLAB. This particular system had a frequency separation factor of five which implies a nominal relative heating factor of 2.6. The PWM switching frequency was set to 3 times the highest target frequency in order to produce the three plots shown in Fig. 12. This choice avoids excessive PWM switching losses associated with higher frequencies, and also is sufficiently high to ensure that high frequency harmonics will not cause unwanted heating when driving the low and middle frequency induction targets. Figure 12(a) shows the relative heating factor for the lowest frequency target when driven by both a quantized Marx waveform and a fast PWM waveform. In this case the frequency modulation ratio with respect to target 1, denoted as $M_{f,1}$, is equal to 75. Because of the high switching frequency, PWM produces a superior sinewave, deviating only slightly for low fundamental voltage amplitudes. The quantized Marx waveform, which is made with significantly fewer switching transitions, still manages to stay within about 5% of the nominal heating factor for fundamental voltage amplitudes in the upper two-thirds range. For the intermediate target, shown in Fig. 12(b) the frequency modulation ratio has been reduced by a factor of five to $M_{f,2} = 15$. At this switching frequency the PWM waveform only yields relative heating profiles that lie within 5% for fundamental voltages above $0.4V_{dc}$. Over this range the quantized waveform is generally better. Lastly, Fig. 12(c) has a frequency modulation ratio of only, $M_{f,3} = 3$.

B. Comparing Power Loss Mechanisms

To the extent that the efficiency of these converters is dominated by loss mechanisms that grow with switching frequency, the Marx inverter could in general be more efficient than a PWM inverter in the multi-target induction heating application. As shown in the previous section, for useful fundamental voltages ranging from $.35V_{dc}$ to $1V_{dc}$, a PWM inverter with a frequency modulation ratio of about three times the highest target drive frequency provides comparable target selectivity in terms of relative power dissipation (the effect of harmonic distortion) in comparison to a Marx inverter. For comparable power delivery performance, the full-bridge PWM inverter should be analyzed for an input bus voltage that is approximately three times higher than that for a 7 level quantizer formed from two M=4 Marx inverters.

The following major loss mechanisms will be considered:

1) Conduction losses.
2) Switching loss due to dissipatively charging and discharging the parasitic body diode depletion capacitance.
3) Switching loss due to non-zero turn on and turn off.
4) Gate drive losses.
5) Losses due to capacitive voltage balancing (unique to the Marx converter).

A comparison of the first four losses are shown side by side for both the PWM and Marx cases in Table II. The conduction loss of the Marx converter is clearly

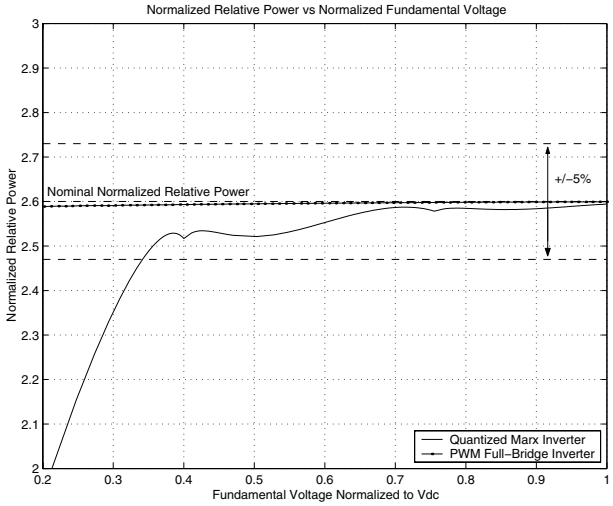

(a) 4kHz Target, $M_{f,1} = 75$.

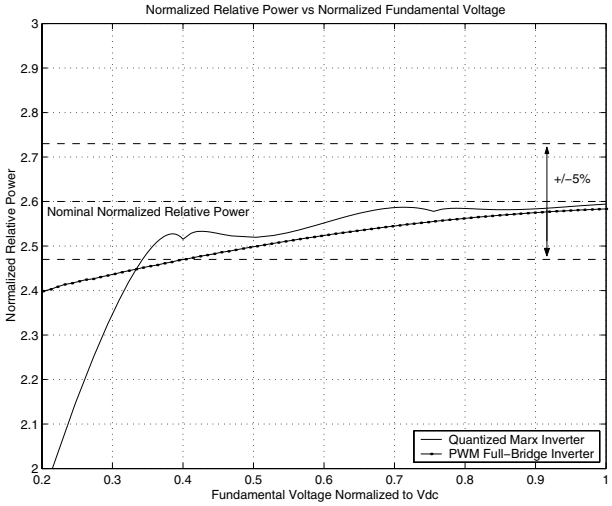

(b) 20kHz Target, $M_{f,2} = 15$.

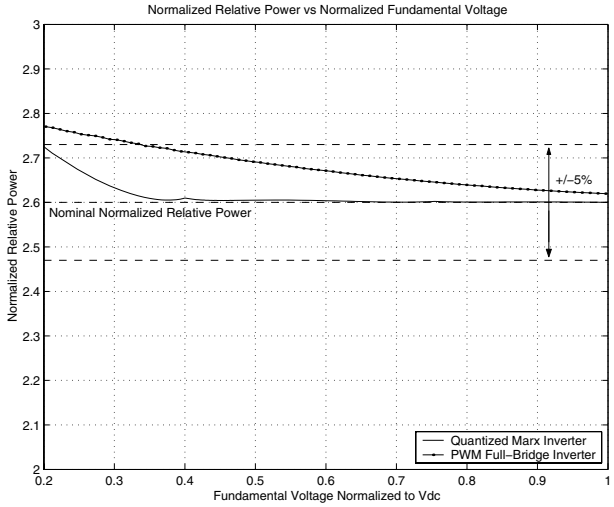

(c) 100kHz Target, $M_{f,3} = 3$.

Fig. 12. Relative heating factor versus normalized fundamental voltage for a three target system.

TABLE II
COMPARISON OF LOSS MECHANISMS.

Loss Mechanism	**PWM Loss**	**Marx Loss (7 levels used)**
Conduction Losses	$I_{rms}^2(2R_{ds,on})$	$I_{rms}^2(6R_{ds,on} + 2R_{ESR})$
Parasitic Diode Capacitance	$4C_{diode}(3V_{dc})^2 M_f f_c$	$16C_{diode}(V_{dc})^2 f_c$
t_{on} and t_{off} switching losses	$\frac{1}{2}[(3V_{dc})(t_{on} + t_{off})f_c] \sum_{t=1}^{4M_f} I(t)$	$\frac{1}{2}[(V_{dc})(t_{on} + t_{off})f_c] \sum_{t=1}^{12} I(t)$
Gate Drive Losses	$4V_{cc}Q_g M_f f_c$	$16V_{cc}Q_g f_c$

worse, since the load current must traverse more switches, and up to an additional two ESR's associated with the Marx capacitors. As a result, the Marx inverter may not be an obvious choice when conduction losses dominate.

However when switching losses dominate, the Marx inverter compares more favorably. The losses associated with charging and discharging the body diode capacitance are reduced by a factor of 6.75. This assumes that this capacitance is linear; the actual nonlinearity of MOSFET body capacitance will lessen this penalty.

The precise calculation of losses due to finite switching speeds requires knowledge of the exact load current value at each switching instant. Of the three load frequencies in our working induction heating example, the Marx inverter executes at most as many load current switch transitions as the PWM inverter when driving the highest frequency target at high voltage. At lower frequencies and voltages, the Marx inverter requires significantly fewer load current switch transitions to create an output waveform with THD comparable or superior to that of the PWM inverter. Even for the highest frequency, highest voltage case, when the number of switching instances for each converter is the same, the full-bridge is penalized by having to switch three times the voltage as the Marx inverter. In terms of the gate drive losses, the Marx converter is 33% higher when all 7 levels are used. When only 5 of the levels are used the gate drive losses become equivalent. In general all switching loss mechanisms in the Marx inverter are reduced when less levels are needed, i.e., 3 levels or 5 levels. Perhaps more significant is the fact that losses improve dramatically when we consider driving the intermediate and lowest frequency targets. In the lower frequency cases, the Marx inverter can operate at an effective switching frequency that is an additional factor of 5 or even 25 times lower than before, while the full-bridge cannot.

The Marx inverter does suffer from an additional loss mechanism not present in the full-bridge. Voltage balancing from capacitor to capacitor incurs dissipation. The conclusions reached in [6] concerning this phenomena also apply here. The energy lost is proportional to the voltage difference between capacitors squared. Furthermore the conclusion that this difference can be minimized by increasing the capacitance, C, or the switching frequency, f_s, also applies here.

V. Conclusions

We are developing a tunable vibration damper that utilizes a thermally responsive gel material to reduce vibrations selectively in a frequency range. The tunable damper relies on the fact that a variable viscosity material can be used to alter the moment of inertia associated with a rotating auxiliary mass. This tuning mechanism can be used alone or in conjunction with other schemes, for example, adjusting the spring constant in the damper, to achieve variable frequency operation.

Thermal activation of each gel-filled compartment in the damper is accomplished using a non-contact induction heating scheme. Each chamber contains an induction target that is designed to exhibit preferential heating at a unique frequency. This multi-frequency, multi-target approach can be used in a wide range of applications, including medical and industrial processes, to provide a wide range of spatial temperature control.

To induction heat these targets, a power supply capable of generating a sum of sinewaves is necessary. A reasonable degree of spectral purity is essential to ensure that unwanted harmonics do not cause undesired power loss in targets meant to be left unexcited. While a conventional PWM inverter could be used, the Marx inverter examined in this paper offers excellent, low harmonic distortion at high efficiencies.

Acknowledgements

The authors gratefully acknowledge the support of the National Science Foundation through a MRSEC grant to MIT's Center for Materials Science and Engineering, a grant from the Grainger Foundation, and support from the Ford Motor Company.

References

[1] Harris C., Crede C.,"Shock and Vibration Handbook (vol.1), McGrawHill, New York, 1961.

[2] Christopher Ting-Kong, "Design of an Adaptive Dynamic Vibration Absorber," *M.eng. Thesis,* Department of Mechanical Engineering, The University of Adelaide, South Australia 5005, April 1999.

[3] F. Forest, E. Laboure, F. Costa, J.Y. Gaspard, "Principle of a multi-load/single converter system for low power induction heating," IEEE Trans. Power Electronics, vol.15, no. 2, pp. 223-230, March 2000.

[4] H. A. Haus, and J. R. Melcher, *Electromagnetic Fields and Energy,* Prentice-Hall, 1989, pp. 446-447.

[5] J.S. Lai and F.Z. Peng, "Multilevel Converters–A New Breed of Power Converters," IEEE Trans. Ind. Applicat., vol. 32, no. 3, pp. 509-517, May/June 1996.

[6] F.Z. Peng, "A Generalized Multilevel Inverter Topology with Self Voltage Balancing," IEEE Trans. Ind. Applicat., vol. 37, no. 2, pp. 611-618, March/April 2001.

[7] A. Nabae, I. Takahashi, and H. Akagi, "A New Neutral-Point-Clamped Inverter", IEEE Trans. Ind. Applicat., vol. IA-17, no. 5, pp. 518-523, Sept./Oct. 1981.

[8] D. Jackson, "Inductively Coupled Power Transfer for Electromechanical Systems," *Ph.D. Thesis,* Massachusetts Institute of Technology, May 1998.

[9] N. Mohan, T. Undeland, W. Robbins, *Power Electronics Converter, Applications, and Design,* Wiley, 1995.

[10] J. Rodriguez,J.-S. Lai, and F.Z. Peng, "Multilevel Inverters: A Survey of Topologies,Controls, and Applications," IEEE Trans. Ind. Electronics, Vol. 49, pp. 724-738, Aug. 2002.

[11] J. Rodriguez, L. Moran, P. Correa, C. Silva, IEEE Trans. Ind. Electronics, Vol. 49, pp. 882-888, Aug. 2002

[12] L. Tolbert, F.-Z. Peng, T. Habetler, IEEE Trans. Ind. Applicat., Vol.35, pp.36-44 Jan./Feb. 1999.

[13] J. Chiasson, L. Tolbert, K. McKenzie and Z. Du Power Electronics Specialists Conference, 2002. pesc 02. 2002 IEEE 33rd Annual, Vol.2, pp503-508, 2002

[14] S. Sirisukprasert; J.-S. Lai; T.-H. Liu IEEE Trans. Ind. Electronics, Vol.49, pp.875-881, Aug. 2002

[15] D. G. Holmes, "A General Analytical Method for Determining the Theoretical Harmonic Components of Carrier Based PWM Strategies," Industry Applications Conference, 1998. Thirty-Third IAS Annual Meeting. The 1998 IEEE, vol.2, pp. 1207-1214